

# Robust frequency control in a standalone microgrid: An adaptive fuzzy based fractional order cascade PD-PI approach

Anil Annamraju<sup>1</sup> | Laxman Bhukya | Srikanth Nandiraju

Department of Electrical Engineering,  
 National Institute of Technology  
 Warangal, Warangal, India

## Correspondence

Anil Annamraju, Department of Electrical Engineering, National Institute of Technology Warangal, Warangal, India.  
 Email: ani223kumar@gmail.com

## Abstract

In addition to low system inertia and stochastic nature of the load, the intermittent nature of renewable output power causes hefty frequency deviations in a standalone microgrid (SMG) that lead to weakening and blackout of SMG. Hence in the SMG, the frequency control issue is always a challenging issue for the operators. To enhance the frequency stability of MG, the control action needs to be more efficient and robust. To answer the above challenge, in this article, a novel adaptive fuzzy based fractional order cascade PD-PI controller is proposed for frequency control of SMG. The proposed controller inherits the merits of both fuzzy and fractional order cascade PD-PI controllers by ignoring the individual limitations. The parameters of the proposed controller are tuned using a recently developed future search algorithm. The proposed controller is tested against various load and renewable disturbances on a real-time MG test system. The simulation outcomes reveal that the proposed controller and algorithm enhance the dynamic response of SMG significantly compared to various powerful controllers in the literature. Moreover, the proposed controller performance is more robust to the uncertainties in the MG and energy storage system as compared to the various robust controllers in the literature.

## KEY WORDS

fractional order cascade PD-PI controller, frequency control, future search algorithm, microgrid, parametric uncertainties, renewable energy sources

## 1 | INTRODUCTION

In the present modern power system scenario, power supply from conventional power sources to remote locations and islands is costly, low reliable, and environmentally hazardous.<sup>1</sup> Microgrids (MGs) are an economical and dependable power solution for such conditions. Based on operational flexibility, MG can operate in two modes, that is, islanded

**ABBREVIATIONS:** AFFOCPID, adaptive fuzzy based FOCPID; CPID, cascade proportional derivative-proportional integral; ESS, energy storage system; FLA, fuzzy logic approach; FLC, fuzzy logic controller; FOCPID, fractional order CPID; FSA, future search algorithm; IOCPID, integer order CPID; MFs, membership functions; MG, microgrid; NB, negative big; NM, negative medium; PB, positive big; PID, proportional integral derivative; PM, positive medium; POS, peak overshoot; PUS, peak undershoot; RES, renewable energy sources; SMG, standalone microgrid; ZE, zero.

and grid-connected mode.<sup>2</sup> Because of the low system inertia and intrinsic characteristics of renewable energy sources (RES), the MG frequency control is difficult in islanded mode compared to the grid-connected mode. Generally, the initial frequency support is obtained from the main grid in the case of grid-connected mode. As a result, the standalone microgrid (SMG) requires a robust, intelligent, and efficient frequency control mechanism.<sup>3</sup>

In the literature, for control engineering problems, several authors proposed various artificial intelligence (AI) based controllers for nonlinear systems.<sup>4-6</sup> Li and Li<sup>4</sup> proposed saturated PI controller, which empirically tunes the parameters of the PI controller with any optimization technique and without precise information of the plant only by using tracking error and saturated input information. Similarly, Khan et al.<sup>5</sup> proposed the beetle antennae search (BAS) algorithm based recurrent neural network, for simultaneous tracking control and obstacle avoidance of a redundant manipulator. Khan et al.<sup>6</sup> proposed BAS for the optimization of the portfolio selection problem. Similarly, Khan et al.<sup>7,8</sup> proposed Zeroing neural network with the BAS algorithm for cooperative mobile manipulators for smart home applications. In Reference 9, Khan and Li proposed a gated recurrent unit with a hyperband algorithm based control framework for the wall-following robot. From the literature, it has been observed that the application of AI techniques to real word control engineering problems attains much attention from control engineers. Keeping in this view, a broad literature review on the application of AI-based robust PI/PID controllers for frequency control of SMG had been performed.<sup>10-17</sup>

In References 10-14, the authors proposed various swarm-intelligent based PID controllers. Das et al.<sup>10</sup> developed genetic algorithm (GA) optimized PID controller, Srinivasaratnam et al.<sup>11</sup> developed grey wolf optimization (GWO) algorithm tuned PID controller, El-Fergany and El-Hameed<sup>12</sup> proposed the social spider optimization algorithm (SSO), Annamraju and Nandiraju<sup>13</sup> introduced the grasshopper optimization algorithm (GOA) based PID controller, in Reference 14, Shankar et al. developed a fruit fly optimized PID controller for frequency control of SMG. The limitation with the swarm-intelligent PID controller is most of the performance of the algorithms depends on their algorithm-specific parameters. To overcome the limitations in these controllers, several authors proposed various PID controllers based on fuzzy and artificial neural networks (ANN).<sup>15-17</sup> In Reference 15, Bevrani et al. recommended a fuzzy-based PI controller, in Reference 16, Sahu et al. proposed a fuzzy based PID controller for frequency control of SMG. In Reference 17, Bevrani et al. proposed the ANN-based PID controller. In addition to these controllers, several authors proposed model based control schemes.<sup>18,19</sup> In Reference 18, Veronica and Kumar proposed internal model control (IMC) based PID controller, in Reference 19, Pahasa and Ngamroo proposed model predictive control based PID controller for SMG frequency control.

The limitation with the PID controller is; its performance highly relies on the optimal trade-off between the integral and derivative part of the PID controller. If the derivative part is dominant it provides better transient performance but it limits the steady-state performance of the MG. On the other hand, if the integral part is dominant it provides better steady-state performance but it limits the transient performance of the system. To overcome this problem in the PID controller, several authors proposed various cascade PD-PI controllers for frequency control of SMG.<sup>20-23</sup> In Reference 20, Khadanga et al. proposed swarm-intelligent based cascade PD-PI controller, in Reference 21, Annamraju and Nandiraju proposed a fuzzy tuned multi-stage PID controller, in Reference 22, Khokhar et al. proposed cascade PI-PD controller, in Reference 23, Khokhar et al. proposed hybrid fuzzy based PD-tilt integral PI controller. From the analysis of these papers, the proposed cascade PD-PI controllers are provided with a better dynamic response than the PID controller. Moreover, the proposed controllers are robust to MG and RES uncertainties.

Although the proposed cascade PD-PI controllers are providing a better dynamic response over PID controllers, it has been observed that a further improvement can be possible by adding the fractional calculus to this cascade PD-PI controller.<sup>24</sup> From the literature, the fractional-order controllers had an added advantage of flexible tuning in integrator and differentiator because of its additional two degrees of freedom in tuning the two additional non-integer knobs (i.e.,  $\lambda$  and  $\mu$ ). But these controllers are certainly underperformed for the variable structure systems like MGs. Moreover, the controller performance is highly dependent on the mathematical model of the system. Certainly, from the literature, FLC can able to provide acceptable performance under these conditions (independent of a mathematical model and unknown nonlinearities of the system). But the performance of FLC highly dependent on selections of rule base and membership functions (MFs). By considering the above factors in the literature, this work proposes an adaptive fuzzy based fractional order cascade PD-PI (AFFOCPID) controller for frequency control of SMG. The motivation for the proposed controller is obtained based on the evaluation of various controllers in the literature as mentioned in Table 1.

From Table 1, the proposed controller aims to meet the following specifications simultaneously by a good frequency controller for modern power system requirements.

TABLE 1 Evaluation of various PID controllers in the literature on LFC analysis of SMG

Controllers	Strengths	Short comes
Optimized PID controllers	<ul style="list-style-type: none"> <li>Simple in structure</li> </ul>	<ul style="list-style-type: none"> <li>Underperformed when an improper trade-off between I &amp; D.</li> <li>A limited degree of freedom in the tuning process.</li> </ul>
Optimized FOPID controllers	<ul style="list-style-type: none"> <li>Additional two degrees of freedom in tuning.</li> <li>Able to handle the known nonlinearities in the system.</li> </ul>	<ul style="list-style-type: none"> <li>Underperformed when an improper trade-off between I &amp; D.</li> <li>Performance is dependent on the exact mathematical model of the system.</li> <li>Uncertain to unknown nonlinearities.</li> </ul>
Fuzzy PID controllers	<ul style="list-style-type: none"> <li>Performance is independent of the mathematical model of the system and unknown nonlinearities in the system.</li> <li>Robust to uncertainties compared to PID and FOPID controllers.</li> <li>Simple in structure.</li> </ul>	<ul style="list-style-type: none"> <li>The performance of the controller is highly dependent on the appropriate MFs range and rule base selection.</li> </ul>
Cascade PD-PI controllers	<ul style="list-style-type: none"> <li>Better dynamic performance over PID controllers due to proper trade-off between I &amp; D.</li> </ul>	<ul style="list-style-type: none"> <li>Performance is dependent on the exact mathematical model of the system.</li> <li>Robust up to a certain extent.</li> </ul>
Proposed AFFOCPID controller	<ul style="list-style-type: none"> <li>The controller is designed to meet all the short comes mentioned in the above controllers (Table 2 explains more regards to this).</li> </ul>	<ul style="list-style-type: none"> <li>The number of variables to be optimized is high.</li> </ul>

TABLE 2 Specifications to be meet by LFC controller

LFC controllers	Specifications of good LFC				
	S <sub>1</sub>	S <sub>2</sub>	S <sub>3</sub>	S <sub>4</sub>	S <sub>5</sub>
Optimal PID	X	X	X	✓	X
Optimal FOPID	X(Moderate)	X	X	✓	X
Fuzzy PID	X	✓	✓	✓	X
Fractional Order Cascade PD-PI	✓	X	X	✓	X (Moderate)
Proposed AFFOCPID	✓	✓	✓	✓	✓

S<sub>1</sub>: Gain the merits of fractional order controller and cascade PD-PI controller.

S<sub>2</sub>: Independent on the mathematical model of the system.

S<sub>3</sub>: Adaptable and flexible in tuning based on the system operating conditions.

S<sub>4</sub>: Robust to RES and load disturbances.

S<sub>5</sub>: Less sensitive to MG & ESS uncertainties.

From Table 1, based on shortcomings of various controllers in the literature and desired qualities of robust and efficient LFC controller, the proposed AFFOCPID controller aims to design the following specifications simultaneously as mentioned in the literature (S<sub>1</sub>–S<sub>5</sub>) and Table 2.

The key contributions of this article are listed below:

1. To mitigate the frequency deviations in SMG, an AFFOCPID controller has been proposed. The proposed controller gains the merits of fractional order, cascade PD-PI and fuzzy logic controllers by ignoring their limits as mentioned in Table 1.
2. The parameters of the proposed controller are optimized by using a recently developed future search algorithm (FSA).
3. Finally, the robustness of the proposed controller is examined by considering concurrent changes in load and RES output power and uncertainties in MG and FC and BES parameters in a single controller framework via a systematic design approach.

4. An attempt has been made to meet all the possible specifications of good LFC ( $S_1$ – $S_5$ ) as stated literature (Table 2) simultaneously.
5. The performance of the proposed controller is evaluated by comparing it with various recently developed controllers in the literature (FSA-PID, FSA-CPID, and FSA-FOCPID)

The work is divided into five sections. Subsequent sections are represented as follows: Section 2 describes the mathematical model of MG. Section 3 illustrates the basic information of FO and proposed fuzzy cascade PD-PI controllers. Section 4 discusses the simulation results, and Section 5 summarizes the overall conclusions of this study.

## 2 | MATHEMATICAL MODELING AND PROBLEM FORMULATION

Figure 1 illustrates the schematic overview of the test system. This test system consists of a wind turbine generator (WTG), solar power (PV), diesel engine generator (DEG), fuel cells (FCs), battery energy systems (BES), flywheel energy storage system (FESS) and load model. In the present work, both WTG power and PV power are considered as uncontrolled power sources (as disturbances). If these sources participate in frequency control, they have to limit their MPPT output power according to frequency deviations, which hindrance the benefit of renewable usage. In this work, DEGs and FCs are responsible for frequency control. Based on renewable power output and load requirement, the residual power will be balanced by DEGs and FCs by using the proposed controller. The mathematical model of the test system is depicted in Figure 2. The MG power balance equation can be expressed as

$$\Delta P_{Load} = \Delta P_{WTG} + \Delta P_{PV} + \Delta P_{DEG} + \Delta P_{FC} + \Delta P_{BES} + \Delta P_{FESS} \quad (1)$$

The frequency deviation ( $\Delta f$ ) in MG based on generation and load can be expressed as

$$\Delta f = \frac{1}{Ms + D} (\Delta P_{DEG} + \Delta P_{WTG} + \Delta P_{PV} + \Delta P_{FC} - \Delta P_{BES} - \Delta P_{FESS} - \beta \Delta f - \Delta P_L) \quad (2)$$

where

The change in DEG power ( $\Delta P_{DEG}$ ) can be expressed as

$$\frac{\Delta P_{DEG}}{U_c} = \frac{1}{s^2 * T_1 * T_2 + s * (T_1 + T_2) + 1} * \frac{1}{1 + sT_3} \quad (3)$$

### TEST MICROGRID

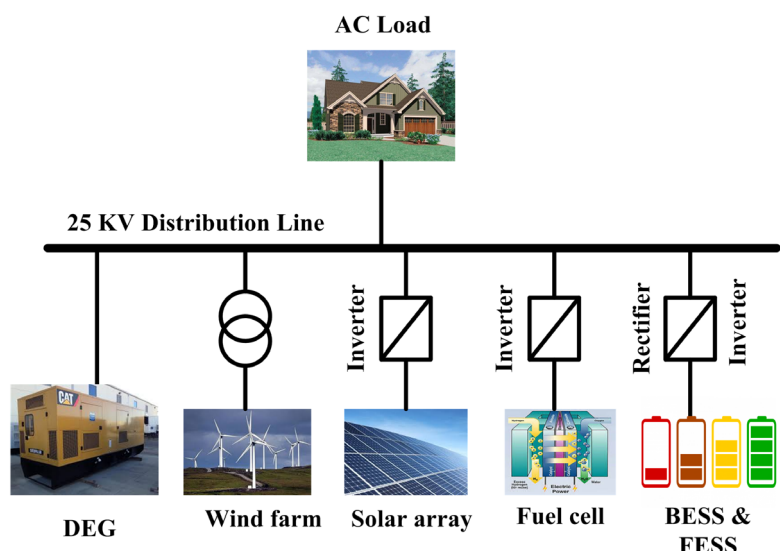
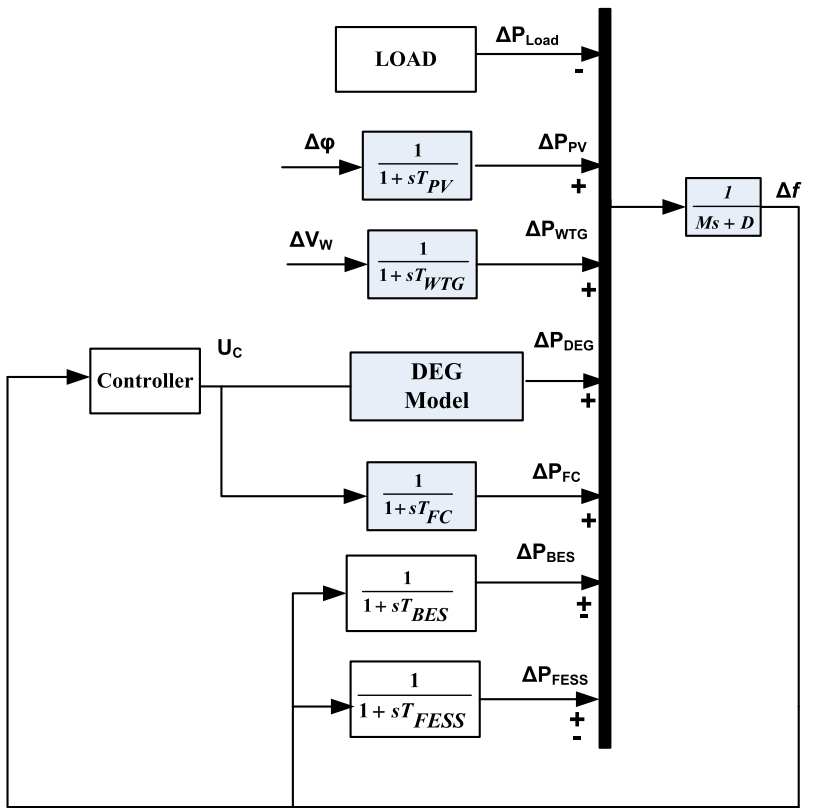


FIGURE 1 The schematic model of the test system

FIGURE 2 Mathematical model of the test system



The change in output power of WTG ( $\Delta P_{WTG}$ ) can be written as<sup>25</sup>

$$\frac{\Delta P_{WTG}}{\Delta V_W} = \frac{1}{1 + sT_{WTG}} \quad (4)$$

The change in output power of solar PV ( $\Delta P_{PV}$ ) can be written as<sup>25</sup>

$$\frac{\Delta P_{PV}}{\Delta \varphi} = \frac{1}{1 + sT_{PV}} \quad (5)$$

where  $T_{WTG}$  and  $T_{PV}$  denotes the conversion time constants of wind and solar systems respectively.

The change in battery power ( $\Delta P_{BES}$ ) output power can be written as<sup>25</sup>

$$\frac{\Delta P_{BES}}{\Delta f} = \frac{1}{1 + sT_{BES}} \quad (6)$$

The change in FESS power ( $\Delta P_{FESS}$ ) output power can be written as<sup>25</sup>

$$\frac{\Delta P_{FESS}}{\Delta f} = \frac{1}{1 + sT_{FESS}} \quad (7)$$

The change in output power of a fuel cell ( $\Delta P_{FC}$ ) can be written as<sup>25</sup>

$$\frac{\Delta P_{FC}}{U_c} = \frac{1}{1 + sT_{FC}} \quad (8)$$

where  $T_{BES}$ ,  $T_{FESS}$ , and  $T_{FC}$  denotes the conversion time constants of battery, flywheel and fuel cells. The test system parameters are given in Table 3.<sup>3,26</sup>

Parameter	Value	Parameter	Value
$M$ (s)	0.1667	$T_{FC}$ (s)	4
$D$ (puMW/Hz)	0.015	$T_{PV}$ (s)	1.8
$T_1$ (s)	0.025	$T_{WTG}$ (s)	2
$T_2, T_3$ (s)	2,3	$T_{BES}$ (s), $T_{FESS}$ (s)	0.1

TABLE 3 MG simulation parameters

### 3 | DESIGN OF PROPOSED AFFOCPID CONTROLLER AND MATHEMATICAL BACKGROUND

### 3.1 | FOCPID controller

The fractional calculus is a standout among the vital branches of the calculus in which the order of the differential and integral parameters is a non-integer value. Recently, fractional calculus is applied successfully to several engineering complications. A detailed analysis concerning fractional calculus is available in Reference 27. Fractional calculus has various definition, namely, Riemann–Liouville (RL), Grünwald–Letnikov (GL), and Cauchy integral formula are applied to define the fractional-order control.<sup>28</sup>

$$DO_{t_0}^r f_x(t) = \frac{1}{r(m-r)} \int_0^t \frac{D^m f_x(t)}{(t-T)^{r+1-m}} dt, \quad r \in R^+, \quad m \in Z^+ \text{ and } m-1 \leq r < m \quad (9)$$

where  $D^m f_x(t)$  is the  $m$ th derivative of function  $f(t)$ . “ $DO_t^r$ ” denotes fractional-order differential operator (a combined differentiator/integrator). “ $DO_t^r$ ” for the function  $f(t)$  of order  $r \in R$  that generalizes the notation for derivatives ( $r > 0$ ) and integrals ( $r < 0$ ). It can be defined as

$$DO_i^r f_x(t) = \begin{cases} \frac{d^r}{dt^r} f(t); & r > 0 \\ f(t); & r = 0 \\ \int_0^t f(T) dT^r; & r < 0 \end{cases} \quad (10)$$

As stated in the literature, the limitation in the PID controller can be overcome with a cascade PD-PI controller. But, the limited degree of freedom in integrator and differentiator (i.e., in Figure 3,  $\lambda$  and  $\mu = 1$ ) limits the maximum performance of cascade PD-PI controller. This problem can be overcome with a fractional order cascade PD-PI controller (FOCPID).

The control signal fed to the FOCPID controller can be expressed as:

$$U_c = \left( K_P + K_D * \frac{s^\mu N}{1 + s^\mu} \right) \left( K_{PP} + \frac{K_I}{s^\lambda} \right) * \Delta f \quad (11)$$

Figure 3 depicts the structure of the FOCPID controller. In the first stage, the error signal fed to fractional order PD controller, later in the second stage to fractional order PI controller. The proposed structure obtains an optimal performance by attaining an optimal trade-off between derivative and integral controllers. The detailed information regards to fractional order PD-PI controller for the LFC problem is available in Reference 24.

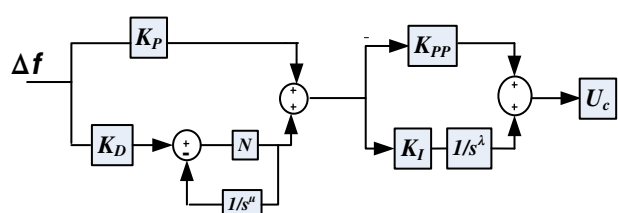
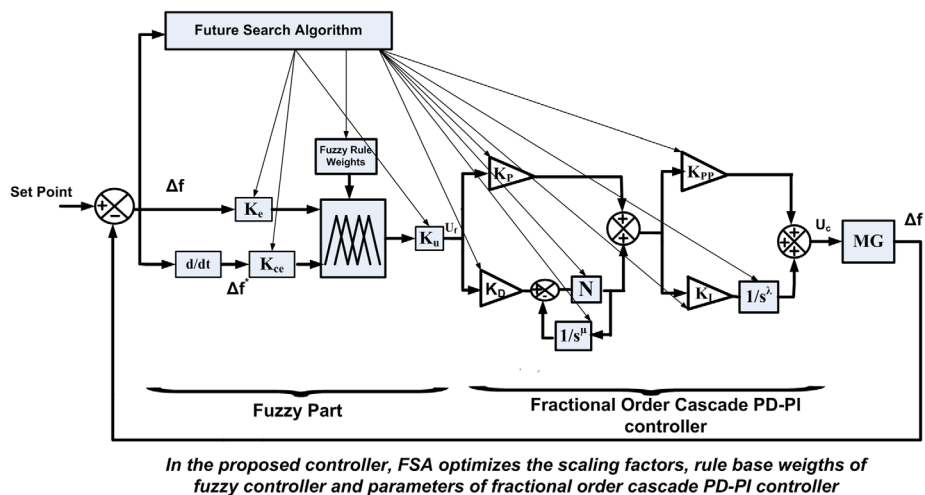


FIGURE 3 Mathematical model of proposed FOCPID controller

**FIGURE 4** Structure of AFFOCPID controller



From (11), compared to the IOCPID controller, the FOCPID controller had an added advantage of flexible tuning in integrator and differentiator (i.e.,  $\lambda$  and  $\mu$ ). As shown in Figure 3, by the use of FOCPID, flexibility is added in the design of the controller and permits to control of real-world process more accurately.

### 3.2 | AFFOCPID controller

The conventional PID, FOPID, fractional-order cascade PD-PI (FOCPID) controllers are efficient when the number of nonlinearities in the system is limited and an exact mathematical model of the system is available. For rapid changes in the operating points due to RES and ESS uncertainties, these controllers may not provide the optimal performance. For such conditions, FLA has proven its efficiency in handling uncertainties.<sup>29</sup> To gain the benefits of both cascade PD-PI controller and FLC, this article proposes a novel adaptive fuzzy based fractional order cascade PD-PI controller (AFFOCPID). Figure 4 depicts the designed structure of the proposed AFFOCPID controller for LFC analysis of SMG. As depicted in Figure 4, two steps are needed to be performed for designing the proposed controller: (1) tuning the FLC inputs and output scaling factors and rule weights of FLA, (2) tuning the parameters of the FOCPID controller. To perform these steps, a recently developed FSA was employed. The detailed explanations regard to various fuzzy stages are listed below.

#### 3.2.1 | Input and output variables for the FLC

The present fuzzy approach has two inputs;  $\Delta f$  and  $\Delta f^*$  and one output, that is, the desired command signal ( $U_f$ ) to the AFFOCPID controller.

#### 3.2.2 | Fuzzy linguistic variables (fuzzification)

Figure 5 depicts the MFs of inputs and output of FLC. MFs are linguistic variables used to convert the crisp inputs and output into fuzzy variables. There are five linguistic variables used to map the inputs and output of FLC. The MFs ranges from NB to PB having centroids at  $-1, -0.5, 0, 0.5, 1$ , respectively are used to map the  $\Delta f$ ,  $\Delta f^*$ , and  $U_f$ .<sup>30</sup>

#### 3.2.3 | Fuzzy rule base design (inference engine)

A total of 25 ( $5^2$ ) rules are framed with two inputs using seven fuzzy sets to resemble the various operating conditions of the system as stated in Table 4. The few control rules of FLC can be described as

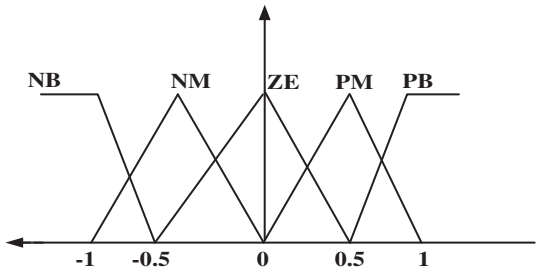
FIGURE 5 Membership functions for  $\Delta f$ ,  $\Delta f^*$ , and  $U_f$ 

TABLE 4 Rule base for FLC

$\Delta f^*$					
$\Delta f$	NB	NM	Z	PM	PB
NB	NB	NB	NB	NM	ZE
NM	NB	NB	NM	ZE	PM
ZE	NB	NM	ZE	PM	PB
PM	NM	ZE	PM	PB	PB
PB	ZE	PM	PB	PB	PB

- Rule  $i$ : If  $\Delta f$  is NB and  $\Delta f^*$  is NB then  $U_f$  is NB with rule weight  $W_i$
- Rule  $j$ : If  $\Delta f$  is NB and  $\Delta f^*$  is NS then  $U_f$  is NB with rule weight  $W_j$

### 3.2.4 | Defuzzification (final crisp output)

Defuzzification is one of the processes of the fuzzy process in which a fuzzy set value transforms into a crisp set value ( $U_f$ ). The defuzzified output (crisp output) based on the centroid method can be expressed as<sup>31</sup>

$$U_f = \frac{\sum_{j=1}^f A_i Q_l}{\sum_{j=1}^f Q_l} \quad (12)$$

where “ $f$ ” denotes the total number of partitions of the fired area,  $A_i$  denotes the total firing area of  $j$  rules, and  $Q_l$  denotes the center of an area.

## 4 | FSA AND ITS APPLICATION TO PROPOSED AFFOCPID CONTROLLER

### 4.1 | Inspiration

The FSA is a recently developed population-based metaheuristic algorithm proposed by Elsisi in the year 2018.<sup>32</sup> It is inspired by basic human behavior. Humans all over the world search for the best life. If any human found that his life is not good, he tries to modify it according to the successful persons in the globe. Based on the human tendency towards the best life, the FSA built by mathematical equations to produce an effective global search mechanism. Each human in the population corresponds to a potential solution in search space. Unless other algorithms, the deployed algorithm is free from algorithm-specific parameters. Besides, the unique features of the proposed algorithm are high local optima avoidance, low complexity and fast convergence.<sup>33</sup> Most of the optimization algorithms update their random initial solution, either by using a local best solution or a global best solution. But these algorithms take a more number of iterations and large computational time due to complex mathematical equations. The FSA is free from the above complexities; hence, FSA is the best option to tune the parameters of the proposed AFFOCPID controller. The detailed mathematical modeling of FSA and its application to the proposed controller is described in the following sections.

## 4.2 | Mathematical modeling

### 4.2.1 | Initialization

To initialize the search process, a population of “ $P$ ” humans is generated in a  $d$ -dimensional search space with the lower bound ( $lb$ ) and upper bound ( $ub$ ) limits. The random solution of each human in the population can be generated by using (13).

$$X(i, :) = lb + (ub - lb) * \text{rand}(1, d) \quad (13)$$

where “ $i$ ” is the present solution of population size;  $X$  denotes solution;  $\text{rand}$  is the uniformly distributed random numbers.

Upon generation of random solutions, each solution in the population is considered as a local solution (LS) and the best one in the population is considered as the global solution (GS) and then the FSA algorithm starts the iterations for finding the optimal solution.

### 4.2.2 | Identification of LS and GS (exploitation and exploration)

The FSA characterizes the solution of every person in the population size by using the following equation which relies upon LS and GS.

Primarily, the search is confined to each country depends on LS which resembles the exploitation characteristics of the algorithm which can be computed as mentioned in (14):

$$X(i, :)_L = (LS(i, :) - X(i, :)) * \text{rand}() \quad (14)$$

Second, the search is expanded to a global level depends on GS which resembles the exploration characteristics of the algorithm which can be computed as mentioned in (15):

$$X(i, :)_G = (GS(i, :) - X(i, :)) * \text{rand}() \quad (15)$$

### 4.2.3 | Population updating

After computing the global and the local convergences, the solution of each person is defined by using (16):

$$X(i, :) = X(i, :) + X(i, :)_L + X(i, :)_G \quad (16)$$

To obtain the balance between exploitation and exploration in the subsequent iterations, Equation (14) is replaced with (17)

$$X(i, :) = GS + (GS - LS(i, :)) * \text{rand}() \quad (17)$$

Based on (17), the algorithm checks the updated GS and LS. If they are better than the old one replaces it otherwise keep the old one. The population updating is repeated either the error tolerance reached a tolerance value or the iteration count reaches to maximum iteration number.

## 4.3 | Objective function formulation

To optimize the parameters of the proposed AFFOCPID controller, it is desirable to define a fitness function to be minimized. In this regard, an ITAE based objective function is chosen in this study. In the control system several error functions are available viz. integral square error (ISE) and integral absolute error (IAE). Among them, an ITAE standard is more

popular and best suitable for frequency control studies.<sup>34</sup> The ITAE standard can be written as

$$\text{ITAE} = \min \text{.of} \int_0^{t_{sim}} t * |\Delta f| dt \quad (18)$$

Subjected to the optimization of controller parameters as mentioned in (19)–(23):

$$0 \leq K_P, K_{PP}, K_I, K_D \leq 5 \quad (19)$$

$$0 \leq N \leq 400 \quad (20)$$

$$0 \leq \lambda, \mu \leq 1 \quad (21)$$

$$0 \leq K_e, K_{ce}, K_u \leq 1 \quad (22)$$

$$0 \leq \text{rule weights}(W_j) \leq 1 \quad (j = 1, 2, \dots, 25) \quad (23)$$

#### 4.4 | Sequential steps for optimization of proposed AFFOCPID controller with FSA

The sequential steps for tuning the proposed AFFOCPID controller with FSA are explained in detail below:

*Step 1: Initialization.* Generate the random population using (14).

Where,  $lb = [0 \ 0 \ 0 \ zeros(1,25) \ 0 \ 0 \ 0 \ 0 \ 0 \ 0 \ 0 \ 0 \ 0 \ 0 \ 0 \ 0]$   
 $ub = [1 \ 1 \ 1 \ ones(1,25) \ 5 \ 5 \ 400 \ 1 \ 5 \ 5 \ 1]$  (24)

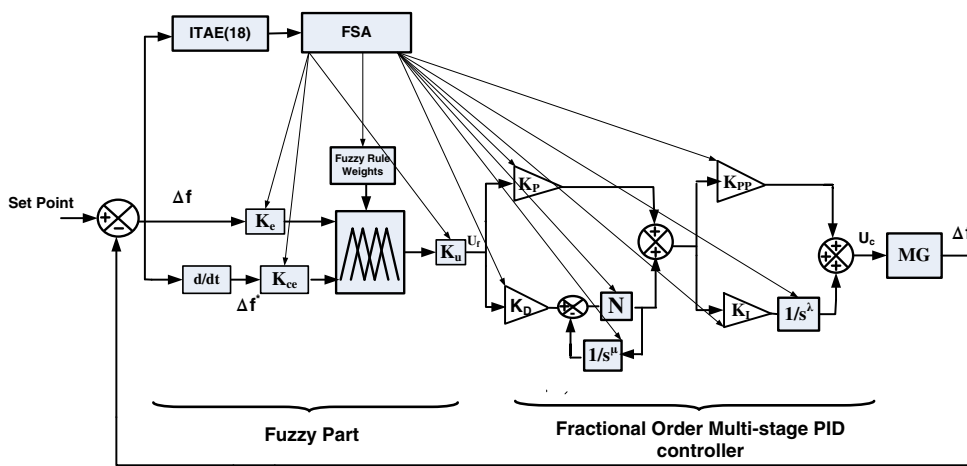


As there are 35 controller parameters identified with the proposed controller, therefore the population size is considered as  $100 \times 35$ . In this 100 represents the number of humans and 35 represents the dimension of search space.

*Step 2: Fitness evaluation.* Run the designed model by implementing the ITAE function as a fitness function to evaluate the performance of the entire population using (18).

**Step 3: Selection.** According to the ITAE value, identify the LS and GS in the population.

*Step 4: Computation of local and global convergence.* Calculate the local and global convergence using (14) and (15).



**In the proposed controller, FSA optimizes the scaling factors, rule base weights of fuzzy controller and parameters of fractional order multi-stage PID controller**

**FIGURE 6** Flow chart for parameters optimization of the proposed controller with FSA

Step 5. Define a new population based on (16) and update GS, LS.

Step 6: *Update the population.* Update the population for the next iterations using (17).

Step 7: *Termination criteria.* Once the iteration count reaches the maximum iteration, the best solution based on the ITAE value is considered as the best set of controller parameters. Display the optimal values of the AFFOCPID controller.

Figure 6 illustrates the flow chart for the optimization of the proposed controller with FSA.

## 5 | RESULTS AND DISCUSSION

In this section, the frequency dynamics of SMG is analyzed under different operating scenarios. The frequency response of SMG with load, renewable and ESS uncertainties are obtained and compared with the proposed AFFOCPID controller, FOCPID controller, CPID controller, and PID controllers. For a fair comparison, the parameters of all controllers are optimized using a recently developed FSA algorithm. The population size of the algorithm ( $P$ ) is 100 and the number of iterations is 50. All the simulations have been carried out on a personal computer system having, 8 GB RAM, Intel Core i7 processor in the MATLAB 2016 environment.

### Operating scenario 1: Stochastic load disturbance in MG

This scenario investigates the frequency dynamic response of MG obtained against the random load disturbance ( $\Delta P_L$ ). Figure 7(A) depicts the random load pattern in MG, and Figure 7(B,C) shows the frequency deviation response of MG with various controllers. In this analysis, for a better view in results, first FSA-PID, FSA-CPID, and FSA-FOCPID controllers are compared in Figure 7(B). The best controller among them (FSA-FOCPID) is compared with the proposed FSA-AFFOCPID controller in Figure 7(C). Table 5 depicts the quantitative analysis of Figure 7(B,C). From Figure 7(C),

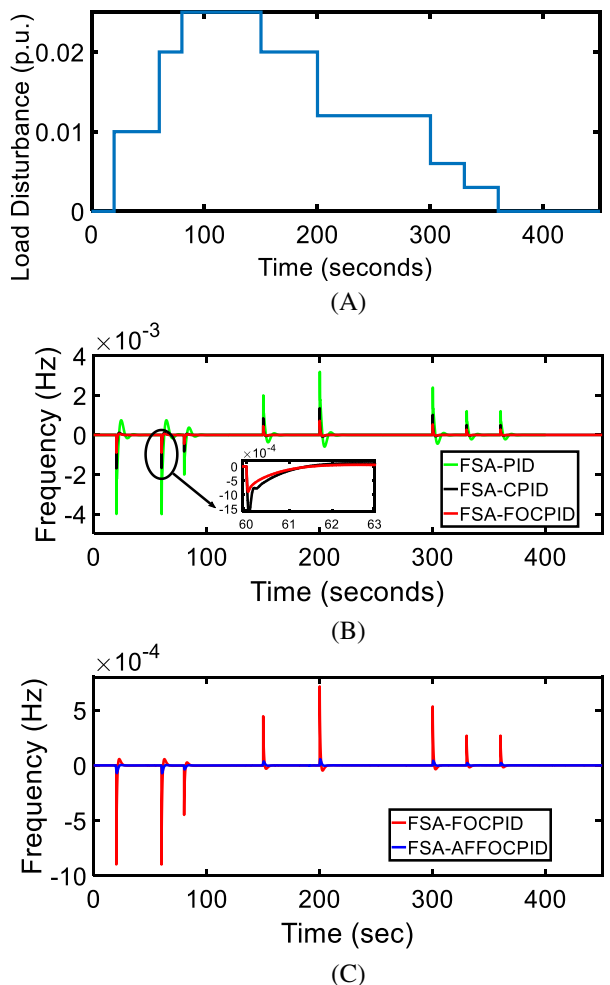


FIGURE 7 (A) Multi-step load disturbances and (B, C) frequency response of MG with various controllers against multi-step load disturbances

it is cleared that, the proposed AFFOCPID controller attains the better dynamic response in terms of less overshoot and fast settling time and low ITAE values compared to various recent controllers in literature. Table 6 denotes the optimized gains of different controllers, and Table 7 denotes the optimized rule weights of the proposed controller. Figure 8 depicts the ITAE performance of the various controllers.

From Figure 8, it is confirmed that the FSA-CPID controller minimizes the frequency deviation error significantly compared to the FSA-PID controller. Hence, it gives a further motivation to proceed in next-level improvement in the

TABLE 5 Quantitative analysis of frequency dynamics of SMG against scenario 1 conditions

Disturbance at various instants	FSA-PID			FSA-CPID			FSA-FOCPID			FSA-AFFOCPID		
	PUS	POS	$T_s$	PUS	POS	$T_s$	PUS	POS	$T_s$	PUS	POS	$T_s$
At $t = 20$ s	-0.004	0.0007	16	-0.0017	0.00015	7	-0.0009	0.00008	5	-0.00012	0	3
At $t = 60$ s	-0.0041	0.0008	17	-0.00168	0.00012	7	-0.0008	0.00006	5	-0.0001	0	4
At $t = 80$ s	-0.002	0.0004	15	-0.0008	0.00001	6	-0.0004	0	5.5	-0.00005	0	3
At $t = 150$ s	-0.0004	0.0019	12	-0.00005	0.0008	7	0	0.00044	6	0	0.00005	3
At $t = 200$ s	-0.0006	0.0035	15	-0.00008	0.0014	9	-0.00005	0.0008	7	0	0.00006	4
At $t = 300$ s	-0.0005	0.0024	16	-0.0006	0.001	8	0	0.00051	6	0	0.00004	4
At $t = 330$ s	-0.0002	0.0012	10	0	0.0005	6	0	0.00025	5	0	0.00002	3
At $t = 360$ s	-0.0002	0.00121	11	0	0.00045	6	0	0.00023	5	0	0.000019	3

TABLE 6 Different gains optimized with FSA for various controllers

Controller parameters	FSA-PID	FSA-CPID	FSA-FOCPID	FSA-AFFOCPID
$K_e$	-	-	-	0.1057
$K_{ce}$	-	-	-	0.1420
$K_u$	-	-	-	0.1665
$K_P$	5	5	4.5614	4.5614
$K_I$	4.8744	4.9910	4.1856	4.1856
$K_D$	4.8570	5	5	5
$N$	21.87	38.9525	287.3958	287.3958
$K_{PP}$	-	4.7373	4.1593	4.1593
$\mu$	-	-	0.1	0.1
$\lambda$	-	-	0.9341	0.9341

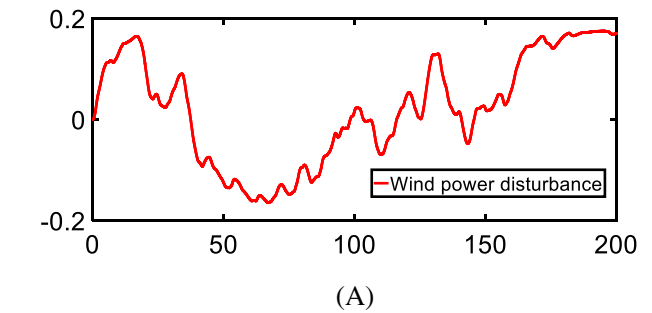
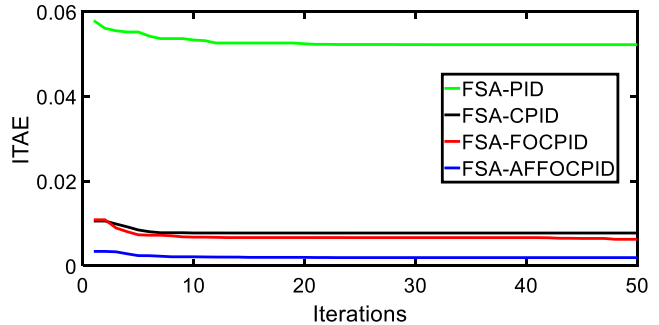
Note: In the proposed controller, in addition to marked parameters, rule base weights also optimized as shown in Table 7.

$W_1$	$W_2$	$W_3$	$W_4$	$W_5$	$W_6$	$W_7$	$W_8$	$W_9$	$W_{10}$
0.6210	0.5737	0.0521	0.9312	0.7287	0.7378	0.0634	0.8604	0.98444	0.8589
$W_{11}$	$W_{12}$	$W_{13}$	$W_{14}$	$W_{15}$	$W_{16}$	$W_{17}$	$W_{18}$	$W_{19}$	$W_{20}$
0.7856	0.5134	0.1776	0.3986	0.1339	0.0309	0.9391	0.3013	0.2955	0.3329
$W_{21}$	$W_{22}$	$W_{23}$	$W_{24}$	$W_{25}$					
0.4671	0.6482	0.0252	0.8422	0.9864					

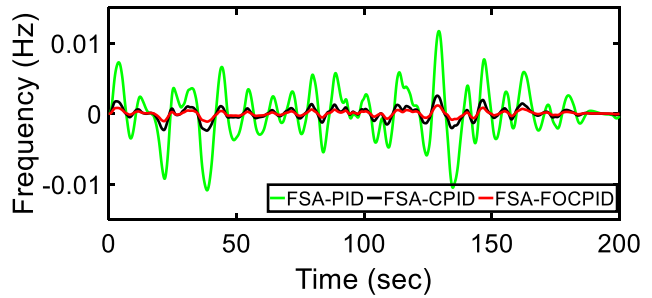
TABLE 7 Rule weights for the proposed AFFOCPID controller

FSA-CPID controller. In this context, fractional calculus is applied to the FSA-CPID controller for further error minimization. The FSA-FOCPID controller minimizes the frequency deviation quite well over the FSA-CPID controller. However, for variable change in structures and uncertainties in mathematical modeling (like in SMG) FLA is an efficient and reliable solution. The combination of FLA and FOCPID controller as proposed in this article (AFFOCPID) controller improves frequency deviation error significantly over FOCPID controller.

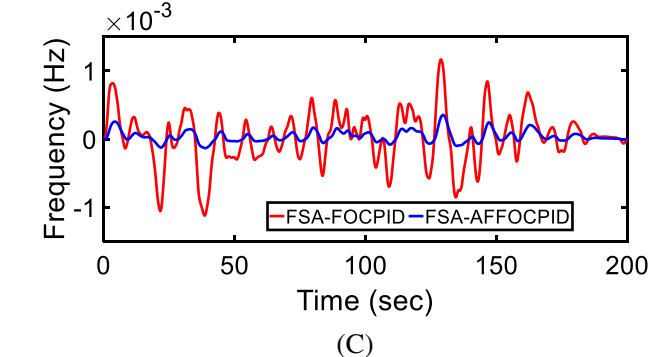
FIGURE 8 ITAE (fitness function) performance characteristics of various controllers with the future search algorithm



(A)



(B)



(C)

FIGURE 9 (A) Wind power disturbances and (B, C) frequency response of MG with various controllers against to wind power disturbances

## Operating scenario 2: Wind power disturbance in SMG

This scenario investigates the frequency dynamic response of MG obtained against wind power disturbance ( $\Delta P_{WTG}$ ). Figure 9(A) depicts the random wind power disturbances in MG, and Figure 9(B,C) shows the MG frequency deviation response with various controllers.

## Operating scenario 3: Solar power disturbance in SMG

This scenario investigates the frequency dynamic response of MG obtained against solar power disturbance ( $\Delta P_{PV}$ ). Figure 10(A) depicts the wind power disturbances in MG, and Figure 10(B,C) shows the MG frequency deviation response with various controllers.

## Operating scenario 4: Multiple disturbances in SMG ( $\Delta P_L + \Delta P_{WTG} + \Delta P_{PV}$ )

This scenario investigates the frequency dynamic response of MG obtained against multiple power disturbances. Figure 11(A) depicts the multiple power disturbances in MG, and Figure 11(B,C) shows the MG frequency deviation response with various controllers.

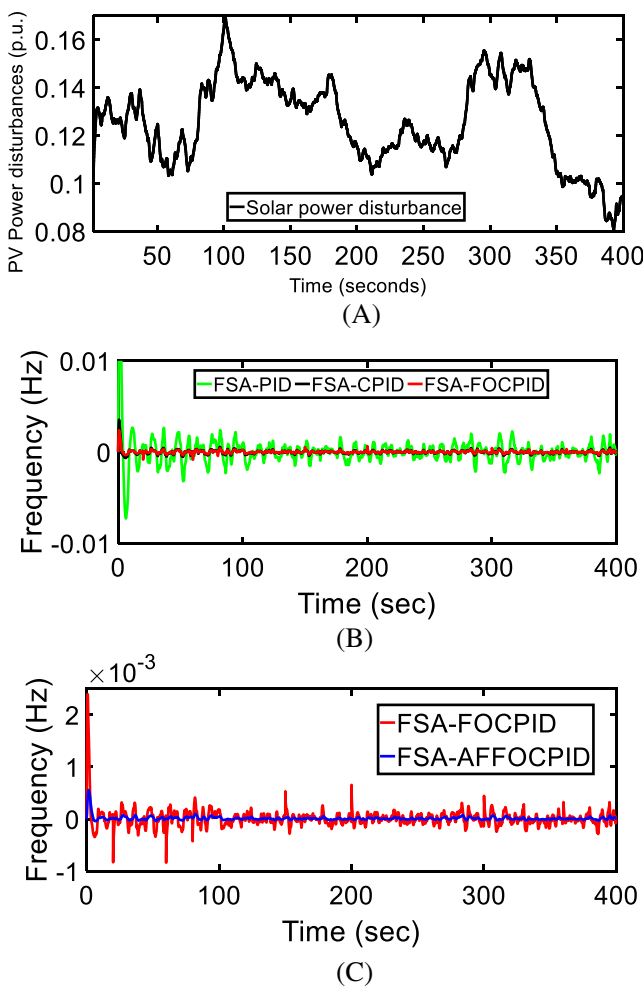


FIGURE 10 (A) Solar power disturbances and (B, C) frequency response of MG with various controllers against solar power disturbances

## Operating scenario 5: Operating scenario 4 + MG uncertainties + ESS uncertainties

This scenario aims to investigate the robustness of the proposed controller over other controllers against multiple disturbances, MG, and ESS uncertainties. Table 8 denotes the percentage uncertainties in MG and ESS. Figure 12(A,B) depicts the MG frequency deviation response against scenario 5 conditions. Table 9 demonstrates the frequency dynamics analysis of various controllers with respect to scenario 4 and scenario 5 conditions.

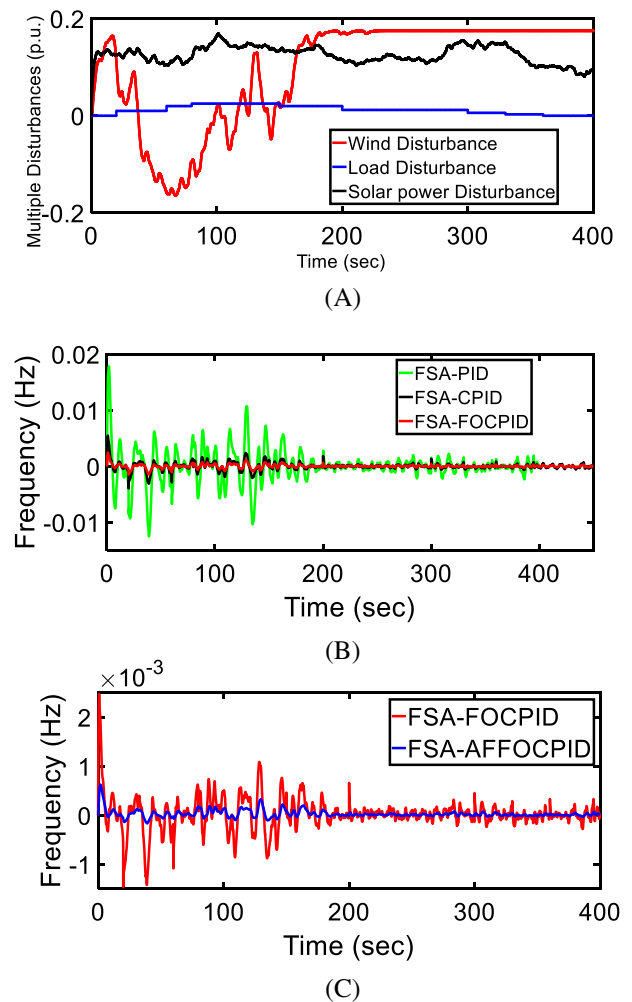
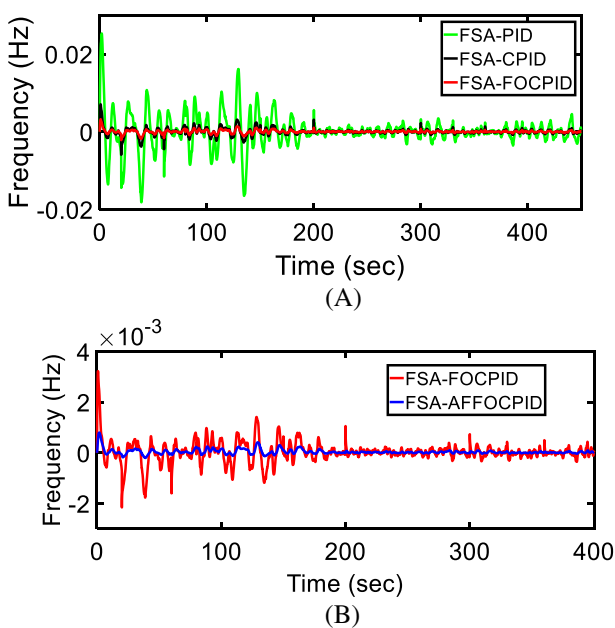


FIGURE 11 (A) Multiple power disturbances and (B, C) frequency response of MG with various controllers against to multiple power disturbances

TABLE 8 Percentage uncertainties in MG and ESSs

MG parameters	
$M$	-50
$R_{AG}$	+40
$D$	-30
$T_1$	+25
ESS parameters (FC and BES)	
$T_{FC}$	+50
$T_{BESS}$	+50
$K_{FC}$	-50
	-50



**FIGURE 12** Multiple power disturbances plus MG uncertainties (A, B) frequency response of MG with various controllers against scenario 5 conditions

**TABLE 9** Quantitative evaluation of various controllers for critical operating scenarios

<b>Methods</b>	<b>PUS</b>		<b>POS</b>		<b>ITAE</b>	
	<b>Scenario 4</b>	<b>Scenario 5</b>	<b>Scenario 4</b>	<b>Scenario 5</b>	<b>Scenario 4</b>	<b>Scenario 5</b>
FSA-PID	-0.011	-0.018	0.019	0.022	0.008	0.12
FSA-CPID	-0.004	-0.006	0.005	0.008	0.0011	0.015
FSA-FOCPID	-0.001	-0.0021	0.0021	0.0036	0.009	0.013
FSA-AFFOCPID	-0.0002	-0.00026	0.0009	0.001	0.004	0.006

## 6 | CONCLUSIONS

This article proposed a novel AFFOCPID controller for frequency control of SMG. A recently developed FSA is used to generate the optimal parameters of the proposed controller. The proposed controller gains the merits of the cascade PD-PI controller, fractional calculus, and fuzzy logic approach due to its effective utilization in a single controller framework. Five different operating scenarios are considered to demonstrate the supremacy of the proposed controller. The simulation outcomes confirm that the proposed controller shows a better dynamic response in terms of fast settling times, less over/undershoots and low ITAE value compared to various recent controllers in the literature. Moreover, the proposed controller is more robust internal MG and ESS uncertainties as compared to the FSA-FOCPID controller, FSA-CPID controller, and FSA-PID controller. As a concluding remark, the proposed AFFOCPID controller met the good LFC prerequisites at a time as modern MG requires. Hence, the proposed controller can be an inevitable solution for complex MG frequency control applications.

## SYMBOLS

- $\Delta P_{Load}$  change in load
- $\Delta P_{WTG}$  change in WTG output power
- $\Delta P_{DEG}$  change in DEG output power
- $\Delta P_{BESS}$  change in BESS power
- $\Delta P_{FESS}$  change in FESS power
- $\Delta P_{FC}$  change in FC power
- $\Delta f$  frequency deviation
- $\Delta f^*$  change in frequency deviation

$R$	speed regulation constant
$D$	damping coefficient
$M$	moment of inertia
$T_G$	time constant of governor
$T_E$	time constant of engine
$T_{PV}$	delay time constant including converter delays also
$T_{WTG}$	delay time constant in WTG system
$T_{BES}$	time constant of battery
$T_{FESS}$	time constant of fuel cell
$T_{FC}$	fuel cell time constant
$\beta$	frequency response characteristics
$U_c$	control signal from the controller to DEG and FC
$K_P$	proportional gain in PD stage
$K_{PP}$	proportional gain in PI stage
$K_I$	integral gain
$K_D$	derivative gain
$K_e, K_{ce}$	scaling factor of fuzzy inputs
$K_u$	scaling factor of fuzzy output
$U_f$	fuzzy output
$N$	filter coefficient
$\lambda$	fractional integral operator
$\mu$	fractional differential operator
$W_j$	rule weight of $j$ th rule
$T_s$	settling time

## CONFLICT OF INTEREST

The authors declare that there is no conflict of interest.

## DATA AVAILABILITY STATEMENT

There are no new data generated in this work. Whatever data used are available openly and cited properly. Moreover, the new findings in this work kept openly.

## ORCID

Anil Annamraju  <https://orcid.org/0000-0001-9358-4348>

## REFERENCES

1. *IEEE guide for design, operation, and integration of distributed resource island systems with electric power systems*; 2011:1-54. IEEE Std 1547.4-2011.
2. Dekker J, Nthontho M, Chowdhury S, Chowdhury SP. Economic analysis of PV/diesel hybrid power systems in different climatic zones of South Africa. *Int J Electr Power Energy Syst*. 2012;40(1):104-112.
3. Bevrani H, Feizi MR, Ataei S. Robust frequency control in an islanded microgrid:  $H_\infty$  and  $\mu$  synthesis approaches. *IEEE Trans Smart Grid*. 2016;7(2):706-717.
4. Li Z, Li S. Saturated PI control for nonlinear system with provable convergence: an optimization perspective. *IEEE Trans Circuits Syst II: Express Briefs*. 2021;68(2):742-746.
5. Khan AH, Cao X, Katsikis VN, et al. Optimal portfolio management for engineering problems using nonconvex cardinality constraint: a computing perspective. *IEEE Access*. 2020;8:57437-57450.
6. Khan AH, Li S, Luo X. Obstacle avoidance and tracking control of redundant robotic manipulator: an RNN-based metaheuristic approach. *IEEE Trans Ind Inform*. 2020;16(7):4670-4680.
7. Khan AT, Li S, Cao X. Control framework for cooperative robots in smart home using bio-inspired neural network. *Measurement*. 2021;167:108253.
8. Khan AR, Khan AT, Salik M, Bakhsh S. An optimally configured HP-GRU model using hyperband for the control of wall following. *Int J Robot Control*. 2021;1(1):66-74.
9. Khan AT, Li S. Human guided cooperative robotic agents in smart home using beetle antennae search. *Sci China Inf Sci*. 2021.
10. Das DC, Roy AK, Sinha N. GA based frequency controller for solar thermal–diesel–wind hybrid energy generation/energy storage system. *Int J Electr Power Energy Syst*. 2012;43(1):262-279.

11. Srinivasaratnam C, Yammani C, Maheswarapu S. Load frequency control of multi-microgrid system considering renewable energy sources using grey wolf optimization. *Smart Sci.* 2019;7(3):198-217.
12. El-Fergany AA, El-Hameed MA. Efficient frequency controllers for autonomous two-area hybrid microgrid system using social-spider optimiser. *IET Gener Transm Distrib.* 2017;11(3):637-648.
13. Annamraju A, Nandiraju S. Frequency control in an autonomous two-area hybrid microgrid using grasshopper optimization-based robust PID controller. Paper presented at: 2018 8th IEEE India International Conference on Power Electronics (IICPE); 2018;1-6; Jaipur, India.
14. Shankar R, Kumar A, Raj U, Chatterjee K. Fruit fly algorithm-based automatic generation control of multiarea interconnected power system with FACTS and AC/DC links in deregulated power environment. *Int Trans Electr Energy Syst.* 2019;29:1-25.
15. Bevrani H, Habibi F, Babahajyani P, Watanabe M, Mitani Y. Intelligent frequency control in an AC microgrid: online PSO-based fuzzy tuning approach. *IEEE Trans Smart Grid.* 2012;3(4):1935-1944.
16. Sahu BK, Pati S, Panda S. Hybrid differential evolution particle swarm optimisation optimised fuzzy proportional-integral derivative controller for automatic generation control of interconnected power system. *IET Gener Transm Distrib.* 2014;8(11):1789-1800.
17. Bevrani H, Habibi F, Shokoohi S. Chapter 12: ANN-based self-tuning frequency control design for an isolated microgrid. In: Vasant P, ed. *Meta-Heuristics Optimization Algorithms in Engineering, Business, Economics, and Finance.* Hershey, PA: IGI Global; 2013:357-385.
18. Veronica AJ, Kumar NS. Load frequency controller design for microgrid using internal model approach. *Int J Renew Energy Res.* 2017;7(2):778-786.
19. Pahasa J, Ngamroo I. Coordinated control of wind turbine blade pitch angle and PHEVs using MPCs for load frequency control of microgrid. *IEEE Syst J.* 2016;10(1):97-105.
20. Khadanga RK, Padhy S, Panda S, Kumar A. Design and analysis of multi-stage PID controller for frequency control in an islanded micro-grid using a novel hybrid whale optimization-pattern search algorithm. *Int J Numer Model Electron Network Dev Field.* 2018;31(5):e2349.
21. Annamraju A, Nandiraju S. A novel fuzzy tuned multistage PID approach for frequency dynamics control in an islanded microgrid. *Int Trans Electr Energy Syst.* 2020;30(12):e12674.
22. Khokhar B, Dahiya S, Singh Parmar KP. A robust cascade controller for load frequency control of a standalone microgrid incorporating electric vehicles. *Electr Power Compon Syst.* 2020;48(6):711-726.
23. Khokhar B, Dahiya S, Parmar K. A novel hybrid fuzzy PD-TID controller for load frequency control of a standalone microgrid. *Arab J Sci Eng.* 2021;46(2):1053-1065.
24. Sahoo P, Mohapatra S, Kumar D, Panda S. Multi verse optimized fractional order PDPI controller for load frequency control. *IETE J Res.* 2020;.
25. Kumar D, Mathur HD, Bhanot S, Bansal RC. Frequency regulation in islanded microgrid considering stochastic model of wind and PV. *Int Trans Electr Energy Syst.* 2019;29(9):e12049.
26. Annamraju A, Nandiraju S. Robust frequency control in an autonomous microgrid: a two-stage adaptive fuzzy approach. *Electr Power Compon Syst.* 2018;46(1):83-94.
27. Monje CA, Chen Y, Vinagre BM, Xue D, Feliu V. Numerical issues and MATLAB implementations for fractional-order control systems. *Fractional-Order Systems and Controls: Fundamentals and Applications.* London: Springer London; 2010:213-256.
28. Dulău M, Gligor A, Dulău T-M. Fractional order controllers versus integer order controllers. *Procedia Eng.* 2017;181:538-545.
29. Annamraju A, Nandiraju S. Robust frequency control in a renewable penetrated power system: an adaptive fractional order-fuzzy approach. *Prot Control Mod Power Syst.* 2019;4(4):181-195.
30. Khezri R, Golshannavaz S, Shokoohi S, Bevrani H. Fuzzy logic based fine-tuning approach for robust load frequency control in a multi-area power system. *Electr Power Compon Syst.* 2016;44(18):2073-2083.
31. Moger T, Dhadbanjan T. Fuzzy logic approach for reactive power coordination in grid connected wind farms to improve steady state voltage stability. *IET Renew Power Gener.* 2017;11(2):351-361.
32. Elsisi M. Future search algorithm for optimization. *Evol Intell.* 2019;12:21-31.
33. Elsisi M, Soliman M. Optimal design of robust resilient automatic voltage regulators. *ISA Trans.* 2021;108:257-268.
34. Guha D, Roy PK, Banerjee S. Load frequency control of large scale power system using quasi-oppositional grey wolf optimization algorithm. *Eng Sci Technol Int J.* 2016;19(4):1693-1713.

**How to cite this article:** Annamraju A, Bhukya L, Nandiraju S. Robust frequency control in a standalone microgrid: An adaptive fuzzy based fractional order cascade PD-PI approach. *Advanced Control for Applications: Engineering and Industrial Systems.* 2021;3:e72. <https://doi.org/10.1002/adc2.72>